TECHNICAL PAPER

JOURNAL OF THE SOUTH AFRICAN INSTITUTION OF CIVIL ENGINEERING

Vol 54 No 1, April 2012, Pages 43–54, Paper 762-2

Mechanistic modelling of weak interlayers in flexible and semi-flexible road pavements: Part 2

M de Beer, J W Maina, F Netterberg

This paper (Part 2 of a two-part set of papers) discusses models and illustrates the adverse effects of weak layers, interlayers, laminations and/or weak interfaces in flexible and semi-flexible pavements, also incorporating lightly cemented layers. The modelling is based on mechanistic analyses for pavement design and evaluation. In Part 1, the effects of these relatively weak layers, interlayers, laminations and/or weak interfaces were discussed. It was shown that methodologies are available to detect and investigate the existence of these weak layers in cemented pavement layers. In Part 2, several cases of the above conditions for different road pavement types are discussed, with field examples. Mechanistic analyses were done on a typical hot mix asphalt (HMA), several cases of a cemented base pavement and a granular base pavement, with and without these weak layers and interface conditions to demonstrate their adverse effects. The analyses focus on the strain energy of distortion (SED) as a pavement response parameter to indicate the potential for structural damage expected within the pavement structure or layer. Generally, the higher the SED, the higher the potential damage in the pavement layer. SED shows some potential for quantifying the relative effects of these weak layers, interlayers, laminations and/or weak interfaces within flexible and semi-flexible pavements.

Note

The 27 photos and 12 figures are numbered continuously throughout Part 1 and Part 2 of this two-part set of papers. However, the references and equation numbers are specific to each part.

INTRODUCTION

Low-strength, weak layers, interlayers, laminations and/or weak interfaces in the upper layers, such as bases and/or subbases, of flexible and semi-flexible road pavements are specifically prohibited in most specifications, as was discussed in detail in Part 1 of this paper (Netterberg & De Beer 2012 – see page 32 of this edition). For detailed definitions of the weak layers etc, and their associated conditions, see Part 1. As discussed in Part 1, premature pavement distress in the form of rippling, arcuate slippage, pumping, cracking or shoving of the bituminous surfacing and shallow base failures of cemented base pavements are not rare in southern Africa (see Photos 1 to 11 in Part 1). It is therefore important to discuss these observations and associated conditions in more detail in order to improve the quality of road construction in southern Africa.

In particular, the aim of Part 2 is to discuss and quantify the adverse effects of weak layers, interlayers, laminations and/or weak interfaces in pavement layers. This is done by means of selected examples of full-scale testing with the heavy vehicle simulator (HVS), including the so-called traffic-associated "crushing failure" found in the top of lightly cemented base layers. The discussion further includes detailed mechanistic analyses of various types of road pavement and interlayer conditions, used (and proposed) here to study the adverse effects of such layers.

As indicated in Part 1, the presence of these layers and/or conditions at any depth in the structural layers of a flexible or semi-flexible pavement (but especially the upper base) can therefore be *quantified, albeit on a relative basis.*

FULL-SCALE HEAVY VEHICLE SIMULATOR (HVS) TESTS ON SELECTED PAVEMENTS WITH CEMENTED LAYERS

Equipment such as the HVS is very useful in identifying the modes of failure of full-scale pavement structures, as is indicated in the following sections.

DR MORRIS DE BEER is a principal researcher at the CSIR Built Environment Unit, and associate editor of the International Journal for Road Materials and Pavement Design (RMPD). He obtained his BSc (Hons), Masters and PhD degrees in Civil Engineering from the University of Pretoria, where he also acts as guest lecturer. He is registered with the Engineering Council of South Africa as a professional engineer, and is a member of SAICE. He also served on various international technical committees, such as the International Society of Weigh in Motion (ISWIM) and Rilem. His research focus is on structural road pavement behaviour, road design, road materials, and vehicle-tyre-road interaction. He is a member of the Transport Infrastructure Engineering group at the CSIR Built Environment Unit.

Contact details:
PO Box 395, CSIR Built Environment
Pretoria, 0001, South Africa
T: +27 12 841 2953
F: +27 12 842 7114
E: mbeer@csir.co.za

DR JAMES MAINA is a chief engineer at the CSIR Built Environment and a Fellow of the South African Academy of Engineering (SAAE). James obtained his BSc (Hons) degree in Civil Engineering from the University of Dar es Salaam in Tanzania, and his Masters and PhD degrees from Miyazaki University in Japan. His research interest is on the development of advanced numerical analysis tools for pavement engineering application. He also leads the Transport Infrastructure Engineering group at the CSIR Built Environment Unit.

Contact details:
PO Box 395, CSIR Built Environment
Pretoria, 0001, South Africa
T: +27 12 841 3956
E: jmaina@csir.co.za

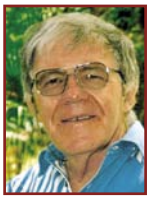

DR FRANK NETTERBERG is an independent researcher and specialist consultant on pavement materials and geotechnics. He graduated from the University of Cape Town with a BSc in Geology in 1960 and a BSc Hons in 1963 and a PhD in 1970 in Engineering Geology from the University of the Witwatersrand, and is a Chartered Engineer and Geologist, a registered Professional Scientist, a Fellow of ICE and SAIEG, and a Member of SAICE and AEG. He has been employed by mining companies, consulting engineers, the CSIR and the University of the Witwatersrand. His research and consulting interests include marginal and unusual materials, pedocretes, soluble salt damage, stabilisation, and active clay roadbeds on which he has published many papers and for which he has received a number of awards.

Contact details:
79 Charles Jackson Street, Weavind Park
Pretoria, 0184, South Africa
T: +27 12 846 7051
F: +27 86 270 8137/8
E: fnetterberg@absamail.co.za

Key words: weak layers, interlayers, modelling, pavement, stabilised

Road P95/1: Bronkhorstspruit – cemented base shallow pavement and poor layer thickness control

Kleyn *et al* (1985) reported on one of the first HVS tests on a shallow but thin (< 100 mm) strongly cemented base pavement on Road P95/1. It was shown that the sensitivity of the pavement increased dramatically when the traffic loading was increased, with a further increase in the rate of deformation when the layers were in a wet state. The layerworks of this pavement were not ideal, as shown in Photo 12 (see Part 1). *It is postulated here that, in addition to the fact that this pavement was of relatively strong but thin and therefore shallow design, the rather poor layerworks (with some weaker layers present) might have influenced the structural performance of this pavement. The former should be seen relative to the behaviour of deeper pavement structures incorporating cemented base/subbase layers, based on the rate of deformation, which was about 50 times lower than that of the shallow pavement above* (Kleyn *et al* 1985, Table 3).

Road P30: Hornsnek – cemented base pavement, interlayer and pumping

Opperman (1984) and later Kleyn *et al* (1985) discussed the structural performance of a strongly cemented gravel base and subbase pavement (Road P30) at Hornsnek, outside of Pretoria. This pavement started pumping after six years in service, and an investigation in 1984 showed the presence of a weak interlayer, unbound and probably a result of poor construction according to Opperman (1984), and not a case of carbonation (for a definition of "deleterious" carbonation in cemented road layers, see Part 1). Photo 1 (see Part 1) indicates the pumping under normal trafficking at that time. In this case, there was a weak interlayer with a thickness of between 25 and 80 mm between the cemented base and subbase, 105 mm to 215 mm from the surface. Owing to its thickness, this weak interlayer was also identifiable with the dynamic cone penetrometer (DCP). During HVS testing in the wet state, severe pumping of fines occurred on the pavement surface from this weaker interlayer, as shown in Photo 16. The cemented base also "collapsed" on the cemented subbase after the weaker interlayer had been "removed" by pumping (Kleyn *et al* 1985, Figure 6). This created a "deeper" pavement structure, demonstrating a "re-balancing" of the pavement under the action of traffic loading, especially in the wetter state. However, this took place at the cost of a rougher pavement surface (maximum deformation > 20 mm within 750 000 standard 40 kN load repetitions in the wet state)

Photo 16 Fine material pumping from HVS test from Road P30 at Hornsnek in 1985 (Opperman 1984)

Photo 17 Failed HVS test section of a cemented base pavement (with 25 mm weak layer at bottom of 80 mm cemented base) after wet test at Hornsnek, Road P30, in 1985 (Opperman 1984)

(Opperman 1984, Figure 8) with an associated lower functional riding quality as shown in Photo 17. *This situation could have been avoided if the weaker layer had not been present in the initial construction of this pavement.*

Asphalt base pavements on lightly cemented base and subbase layers: KwaZulu-Natal

This phenomenon was also observed and modelled during HVS tests on flexible asphalt base pavements, incorporating lightly cemented (C3/C4) subbase layers in KwaZulu-Natal (De Beer 1985, Chapter 5). In a case study by De Beer (1985) with the HVS on Van Reenen's Pass, it was found that the full thickness of a 150 mm upper cemented subbase of an asphalt base pavement was relatively weak and fully carbonated. This particular layer was constructed during snowfalls in 1981, which hampered the construction control on site. This caused a "sandwiched" type of pavement structure, in which this weaker layer dominated the structural fatigue failure of the rather stiff recycled asphalt base of this pavement, even in the dry state (see Photos 18 and 19). Again, this illustrates the adverse effect of a weak layer within the upper supporting pavement layers. In another study De Beer (1985) showed the effect of erosion in the wet state of a cemented Berea Red Sand upper subbase underneath an asphalt base. In this case, a weak layer was created outside the wheel path, between the upper subbase and the asphalt base. In order to avoid

Photo 18 Crack pattern on recycled asphalt base layer on Van Reenen's Pass during HVS testing in 1985 (De Beer 1985)

Photo 19 Fully carbonated and relatively weak upper cementitious subbase layer directly underneath the recycled asphalt base layer, resulting in a "sandwich" structure of a weak upper subbase on the N3 at Van Reenen's Pass (De Beer 1985)

this condition, an erosion test device and associated erodibility criteria were proposed for material design in the laboratory *before* construction (De Beer & Visser 1989).

Road MR27: Stellenbosch to Somerset West – strongly cemented (C2) base pavement

In another case of a relatively strongly cemented base pavement in the Cape, near Stellenbosch and Somerset West, Jordaan (1988) found that weak interlayers developed within the cemented base after traffic loading with the HVS, and also found a second weak interlayer just beneath the surfacing. In addition, crack activity measurements by Rust (1987) complemented the analysis of the traffic-associated failure of this pavement. Photo 20 indicates severe pumping during the HVS test on this road section in the wet condition. In addition, the adverse effect of moisture in the upper layers (i.e. wet state) was also demonstrated here, in that the bearing capacity of this pavement was reduced from 8 million standard axles in the dry state to a mere 1,6 million standard axles in the wet state (Rust 1987). *This is another illustration of the combined action of traffic loading and moisture on these pavements, with reported evidence of weak interlayers.*

Photo 20 Pumping of fines during HVS testing from a strongly cemented (C2) base pavement (Road MR27) (Rust 1987; Jordaan 1988)

Discussion

The above examples (as well as those discussed in Part 1) illustrate the importance of the actual pavement situation in the field versus the pavement structure as designed, specifically the occurrence and effect of weak layers, interlayers, laminations and/or weak interfaces in actual pavement structures. It should also be noted that, once surface failure is initiated for whatever reason, *accelerated pavement failure* occurs. This, of course, is also a strong function of road roughness and associated vehicle suspension, and therefore of axle and tyre dynamics, as indicated by Lourens (1995) and also Steyn (2001). This situation is aggravated when the pavement is in a wet condition. In addition to the examples given above, this accelerated damage progression on various types of pavement has been adequately demonstrated and documented through many years of HVS testing and associated observations of pavement failures in South Africa (Maree 1982; Freeme *et al* 1987; Rust *et al* 1997; Du Plessis *et al* 2008).

To aid in pavement evaluation for the purposes of rehabilitation, Freeme (1983) and Freeme & De Beer (1983) published documents defining the *structural behavioural states* of different flexible and semi-flexible pavement types (by catalogue) to inform engineers about specific evaluation and rehabilitation design strategies (see also Jordaan 1988). These documents demonstrate that relatively weak layers between structural layers in a pavement are highly detrimental to the pavement's structural performance, and become even more crucial in wet conditions, as was discussed above. During wet conditions, the pavement easily changes its structural behaviour into what is referred to as the "moisture accelerated distress" (MAD) state, as reported by De Beer & Horak (1987). In the next section the so-called "crushing failure" of cemented base pavements is discussed.

CRUSHING FAILURE MECHANISM FOUND FOR CEMENTED BASE PAVEMENTS

Effect of tyre–pavement contact stress and associated crushing failure mode of a cemented layer

Lightly cemented base/subbase layers may also suffer from traffic-associated "crushing failure". This failure mode could result from a relatively weak upper portion in cemented bases, but could even occur in relatively dry conditions (De Beer 1990). This "weakness"

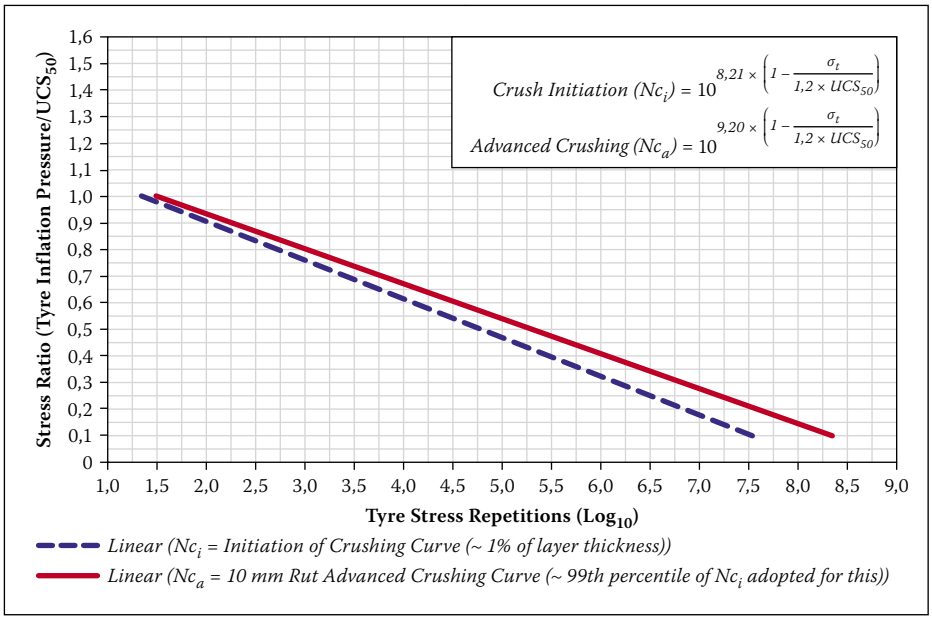

Figure 2 Crushing failure of pavements incorporating lightly cemented base layers (modified from De Beer 1990)

Photo 21 Crushing (dry condition) of a lightly cemented base layer as a direct result of HVS trafficking (De Beer 1990)

Photo 22 Signs of pumping from the cementitious base layer during a wet HVS test, after crushing in the dry state (De Beer 1990)

in the layer is to be seen relative to the applied contact stress it needs to carry from especially truck tyres. In this paper, it is assumed that the tyre inflation pressure is equal to the vertical tyre contact stress. However, a multitude of studies have indicated that three-dimensional (3-D) tyre–pavement contact stresses are not simple, and special provision should ideally be made to incorporate these complex contact stresses into pavement design (De Beer *et al* 1997, 1999, 2002, 2004; De Beer 2006, 2008). In these days of higher tyre inflation pressures (and hence tyre vertical contact stresses of up to 1 000 kPa or more), the importance of avoiding a relatively weak upper base is well illustrated by Equations 1 and 2 (also see Figure 2). Figure 2 and these equations show the empirical relationships found for tyre contact stress-associated crushing failure in terms of the "initiation" of crushing failure (Crush Initiation, Nc_i), as well as "advanced" crushing failure (i.e. Advanced Crushing, Nc_a) (De Beer 1989a, 1989b, 1990; De Beer *et al* 1997, 1999).

Crush Initiation (Nc_i)

$$= 10^{8,21 \times \left(1 - \frac{\sigma_t}{1,2 \times UCS_{50}}\right)} \quad (1)$$

Advanced Crushing (Nc_a)

$$= 10^{9,20 \times \left(1 - \frac{\sigma_t}{1,2 \times UCS_{50}}\right)} \quad (2)$$

Where:

Nc_i = initiation of average crushing life span (units in repetitions of tyre–pavement contact stress, σ_t)

Nc_a = advanced average crushing life span (units in repetitions of tyre–pavement contact stress, σ_t)

σ_t = tyre contact stress (~ tyre inflation pressure in this paper) in kPa

UCS_{50} = *in situ* DCP-derived unconfined compressive strength (UCS) of the top 50 mm of base layer in kPa

The probability for Nc_i = 50%, R^2 = 0,89, n = 23 (De Beer 1990).

For example, Figure 2 indicates that about one pass of a tyre resulting in an average vertical contact stress of σ_t = 1 000 kPa on a cemented base layer would immediately initiate the crushing mode of failure (Nc_i) of the upper base (~ 50 to 75 mm) with a similar *in situ* UCS_{50} strength. Further, a UCS_{50} of about 3 MPa would be needed for 1 million contact stress repetitions before initiation of crushing failure in the upper 50 to 75 mm. The crushing (or compression) failure, even in the dry state, of a cemented base layer, as was observed under HVS testing, is illustrated in Photos 21, 22 and 23. The existing C3 base strength

requirement of UCS = 1,5 MPa (strength in the field) should therefore be adequate to carry about 1 million contact stress repetitions at σ_t = 500 kPa, and approximately 10 000 stress repetitions at a tyre contact stress of σ_t = 1 000 kPa. These relationships (Equations 1 and 2) were empirically derived from DCP tests at HVS sites (De Beer 1990). Further, as stated in the original work on the crushing failure mode, the initiation of crushing in thinly sealed cemented base pavements almost corresponds to the fatigue life of the thin asphaltic surfacing seal (De Beer 1989a, 1990). Advanced crushing (Nc_a) corresponds to approximately 10 mm of deterioration (downward displacement) in the top of the cemented base, which is a strong warning sign of a shallow failure that may need urgent maintenance.

As shown in Part 1, it is therefore concluded that the creation (or existence) of relatively weak (crushed) upper layers, interlayers, laminations and/or interfaces due to any cause *should be avoided at all costs*, even at the expense of other aspects such as the quality of the surface finish.

MECHANISTIC PAVEMENT ANALYSIS WITH AND WITHOUT INTERLAYER SLIP

It is generally accepted that weak layers, laminations and/or weak interfaces of any kind in the upper base layer, including compaction planes, are highly detrimental to the structural and functional performance of a pavement, as shown by their general prohibition in nearly all specifications. Indeed, it can be quantitatively shown on a relative basis, based on the mechanistic pavement analysis methodology, that relatively smooth interfaces (see Photos 6, 7 and 8 in Part 1, and 24 and 25 alongside) and relatively weak interlayers (see Photos 12, 13 and 15 in Part 1) are highly detrimental at any depth in the base layer, and even at depth such as between the base and subbase layers. This is largely due to a redistribution of stresses and strains (or energy) as a direct result of a degree of "imbalance" caused by these weaker layers and/or weak interface conditions (e.g. AUSTROADS 1998; De Beer 1985, Chapter 5; Romanoschi & Metcalf 2001a, 2001b; Nageim & Hakim 1999).

For the case of a weak interface, a simple analogy would be the improved elastic deflection characteristics obtained by glueing the laminations of a laminated timber beam. An extreme analogy, applicable also to horizontal sliding failure in the upper base, would be the difference between a glued and an unglued ream of paper. Both crushing failure of a weak upper base and

Photo 23 Final state of the lightly cemented base layer after HVS testing and crushing, in the wet state (De Beer 1990). Note the amount of material lost from the wheel path in centre of photo

Photo 24 Field cores from lightly cemented base layer – left core: solid; right core: weak interlayers

Photo 25 Signs of delamination (possible construction plane) in a lightly cemented layer (De Beer 1990)

Photo 26 Typical signs of crushing failure in a pothole in a cementitious base pavement

Photo 27 Crushing failure of the top of a lightly cemented base layer – final state of the lightly cemented base layer after some HVS testing

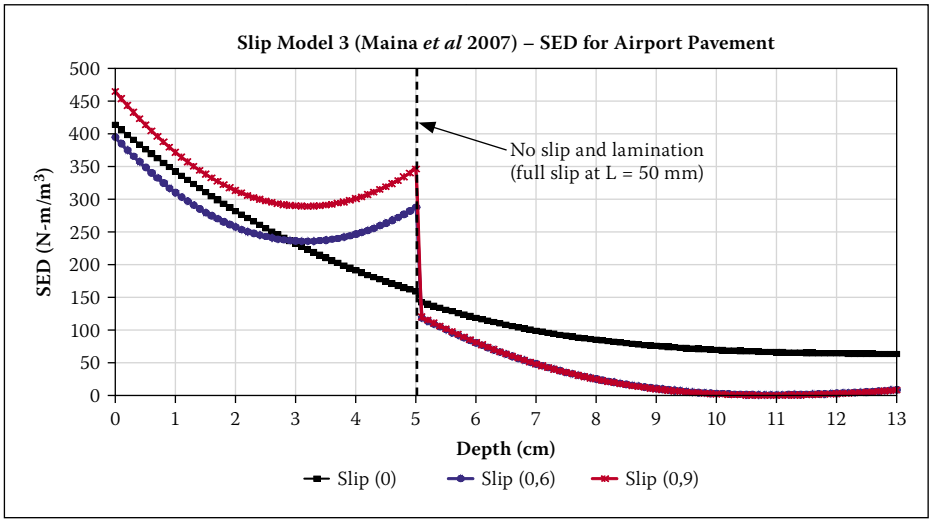

Figure 3 Variation of maximum SED with depth under the front most outside tyre with vertical and horizontal tyre loading on 16 tyres of a Boeing 747-400 – modelled on a typical asphalt base airport pavement with and without lamination at 50 mm depth (after Maina *et al* 2007)

sliding on interfaces between laminations or weak interfaces appear to have contributed to many "shallow" base failures of cemented bases in southern Africa, though both have not necessarily occurred at each failed site.

In the following section examples of various mechanistic analyses show the relative effects of interlayers (weak layers, laminations and/or weak interfaces), based on the theoretical interlayer slip models developed by Maina *et al* (2007). The relative importance of a lamination or weak interface of thickness t ~ 0 versus relatively weak layers, or interlayers of a definite thickness t > 0 versus simple weakening of a layer under the action of trafficking, is discussed using the mechanistic approach.

Strain energy of distortion (SED) as pavement response parameter

According to Timoshenko & Goodier (1951), the quantity of strain energy stored per unit volume of the material can be used as a basis for determining the *limiting stress at which failure occurs.* For this to be applied to isotropic materials, it is important to separate this energy into two parts – one due to the change in volume and the other due to the distortion – and to consider only the second part in determining the strength. Whatever the stress system, failure occurs when the SED reaches a certain limit. The mechanistic analyses discussed in this paper focus on SED as a pavement response parameter in terms of its value as an indicator of potential damage in a pavement layer. Generally, the higher the SED value, the higher the potential for damage in the pavement layer. SED shows some potential for quantifying the relative effect of these deleterious layers/conditions of interlayers in flexible and semi-flexible pavements. Theoretically, according to Timoshenko & Goodier (1951), the total strain energy per unit volume, V_0, is expressed by Hooke's law, as follows:

$$V_0 = \frac{1}{2E}(\sigma_x^2 + \sigma_y^2 + \sigma_z^2) - \frac{\nu}{E}(\sigma_x\sigma_y + \sigma_y\sigma_z + \sigma_z\sigma_x) + \frac{1}{2G}(\tau_{xy}^2 + \tau_{yz}^2 + \tau_{xz}^2) \quad (3)$$

so that SED can then be expressed as follows:

$$SED = V_0 - \frac{1-2\nu}{6E}(\sigma_x + \sigma_y + \sigma_z)^2 \quad (4)$$

Where:

E = Young's Modulus (MPa)
ν = Poison's Ratio
G = shear modulus (MPa)
σ = compressive or tensile stress (MPa)
τ = shear stress (MPa)

Using Equations 3 and 4 it is anticipated that locations within the pavement structural layers that have relatively higher values of SED (i.e. so-called "hot spots") will potentially fail first before points with relatively lower SED values. Note that the unit of SED is N-m/m^3.

Example 1: Pavement type: hot mix asphalt (HMA) base: smooth vs rough interface between top of subbase and bottom of asphalt base – vertical tyre loading only

In this section, an example of a lamination or interface (modelled as "smooth" or "full slip") at the bottom of a typical HMA base airport pavement is demonstrated, relative to the case of full-friction (modelled as "rough" or "no slip") condition by way of mechanistic modelling. Figure 3 shows an evaluation of interlayer slip conditions, i.e. a weak interface, which is modelled as a layer (or boundary condition) without any thickness, t ~ 0, for a typical flexible airport pavement structure (Maina *et al* 2007). For the purpose of this paper, the results of utilising "Slip Model 3" (Equation 13 in Maina *et al* 2007) are given since it seems to be more appropriate than other slip models investigated by Maina *et al* 2007. The variation of SED with depth under the front outermost tyre of a Boeing 747-400 gear (of 16 tyres) (after Maina *et al* 2007) for three slip rate values (indicating the percentage of horizontal movement allowed theoretically) is clearly

Table 1 Pavement structure and associated engineering properties used for the mechanistic analysis – Road Category B, ES3 (TRH 4, COLTO 1996)

Layer *	Thickness (mm)	E modulus (MPa)	Poisson's ratio
Surfacing (S2)	15	1 000	0,44
Cemented base (C3)	50	3 000/30 **	0,35
Cemented base (C3)	75	3 000	0,35
Cemented subbase (C4)	200	1 500	0,35
Selected layer (G7)	150	250	0,35
Subgrade soil	∞	100	0,35

* For material and pavement codes, see TRH 4 (COLTO 1996)

** Representing a relatively weak layer approximated with a rather low effective elastic modulus (i.e. 30 MPa), compared with a "solid" and intact layer with an effective modulus of ~ 3 000 MPa

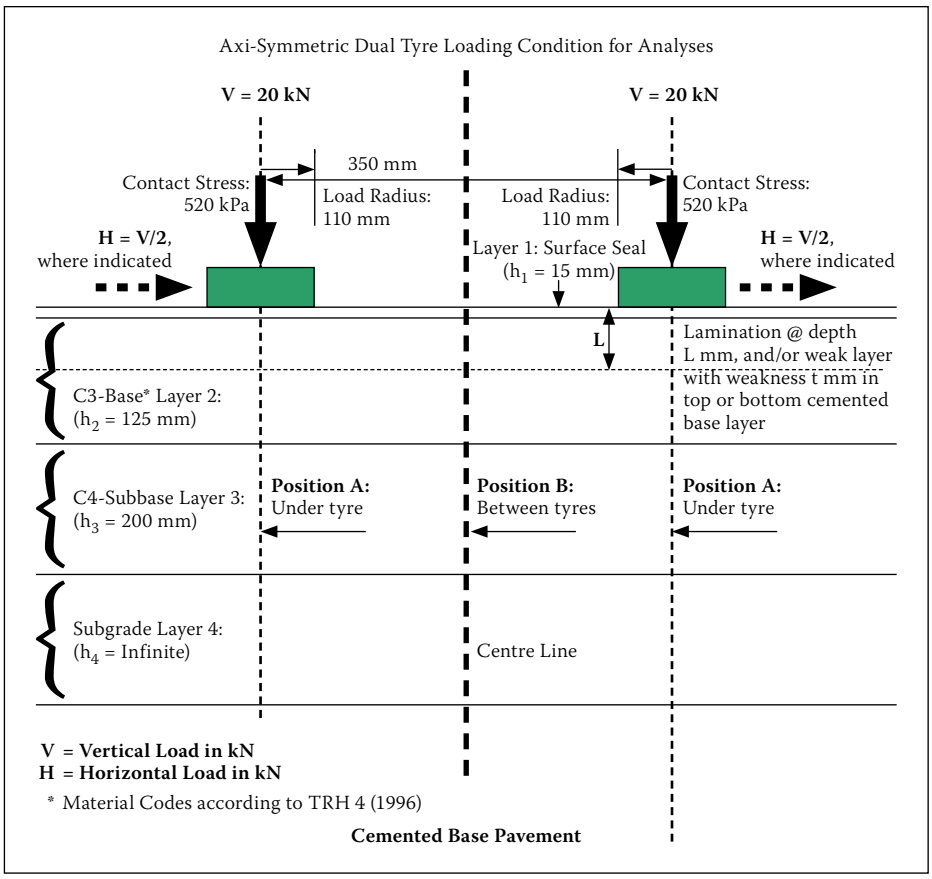

Figure 4 Layout for mechanistic analysis of a cemented base pavement (this study)

shown in Figure 3. The trend of maximum SED indicates that, whatever the slip rate value, relatively higher SED values are found at the surface of the pavement structure. Note that a slip rate of 0,0 represents "full friction" (no slip or full bonding) between subsequent horizontal layers, and a slip rate of 0,9 represents "full slip" (almost no friction or no bonding for practical purposes). Figure 3 shows that as the slip rate increases, SED at the bottom of the top layer (where the interface slip occurs) increases to almost 75% of the SED obtained at the top of the pavement layer and this may result in a potential "bottom-up" failure condition.

Based on the SED analysis, interlayer slip may therefore influence the position and type of potential asphalt layer failures, such as cracking and deformation. Less drastic changes in SED occurred at the bottom of layer 2 as a direct result of the "re-balancing" of the stress and strain distribution within the pavement layers. The effect of this re-balancing is that the potential for distortion (i.e. SED) is shifted to the top layers above the lamination, interface or relatively weaker interlayer.

The general trend in SED with depth in Figure 3 is that, as the slip rate increases, SED tends to decrease through the thickness of the layer up to a certain depth within the asphalt base (in this particular case at a depth of approximately 30 mm), and then starts increasing again towards the bottom of the layer. In summary therefore, damage is expected to occur on the road surface (most probably rutting), as well as from the bottom of the asphalt base (most probably dominated by fatigue cracking, not excluding rutting from the bottom). This theoretical finding, however, needs further field verification.

Example 2: Pavement type: cemented base: smooth vs rough single interface within the cemented base – vertical tyre loading only

In this section an example of a single lamination or weak interface ("smooth" boundary condition, also referred to as "full slip" or "no friction") at a depth of L = 65 mm (i.e. 15 mm + 50 mm) in the cemented base (Road Category B, ES3, TRH 4 dated 1996, see COLTO 1996) is demonstrated. Slip Model 3 from Maina *et al* (2007) was also used for this analysis and the engineering model parameters are given in Table 1. As already indicated, the design capacity of this pavement is ES3 = 3 million standard axles (MISA) over 15 years. Note that MISA = million repetitions of a standard 80 kN axle with four tyres at 520 kPa tyre pressure, as defined in TRH 4 (COLTO 1996).

The load configuration is the standard loading per tyre, which is 20 kN and a value of 520 kPa for the contact stress. The layout of the pavement and its tyre loading used in the mechanistic analysis is illustrated in Figure 4. This figure also shows the different layer thicknesses and the depth of the lamination in the cemented base layer, which was modelled at a depth of L = 65 mm (i.e. 15 mm + 50 mm).

For the purposes of illustration, only one phase (i.e. the initial "pre-cracked" phase) of the structural behaviour of cemented layers is used here (for the different phases in the "life" of a cemented layer, see Theyse *et al* 1996). The SED results with vertical loading (V) only, under one tyre (Figure 4, Position A) and between the dual tyres (Figure 4, Position B) for this pavement condition are illustrated in Figure 5. Note that the various mechanistic analyses were done at two different positions, i.e. under the tyre (Figure 4, Position A) and between two tyres (Figure 4, Position B), and the SED values are reported through the depth of the pavement. Note that the case of vertical tyre loading (V) only, is considered in Figure 5.

The highest relative SED value of approximately 130 N-m/m^3 (see **red**-dot curve) occurs at a position directly underneath the tyres at the depth (L) of the lamination (or weak interface), which is at L = 65 mm, from the surface of the pavement. The position of the second highest SED value (~ 28 N-m/m^3, see

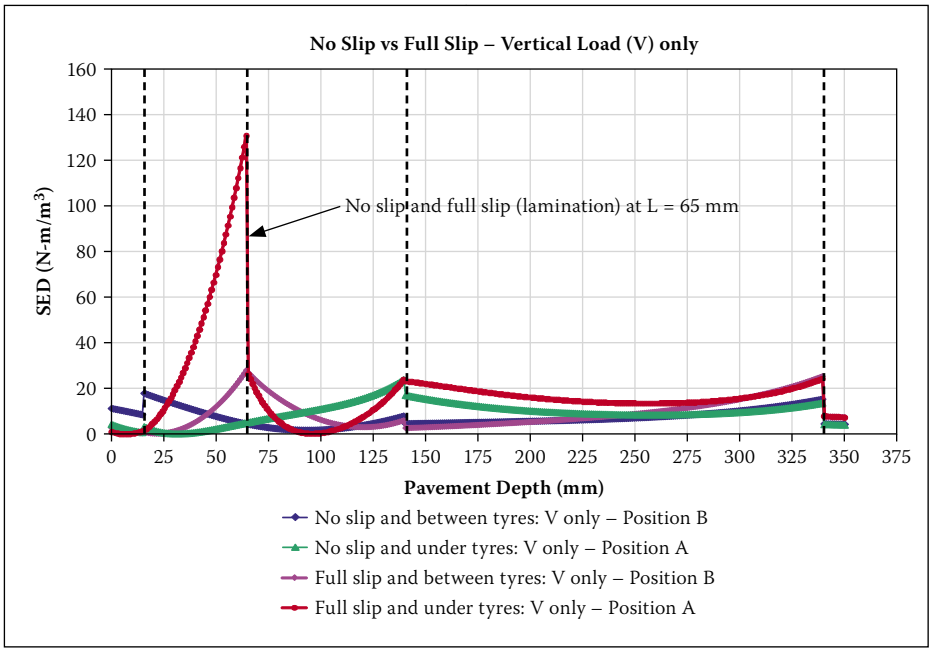

Figure 5 Strain energy of distortion (SED) results of the cemented case pavement. Note the relatively high value of SED at L = 65 mm with full slip (~ single lamination at L = 65 mm) directly under the tyre

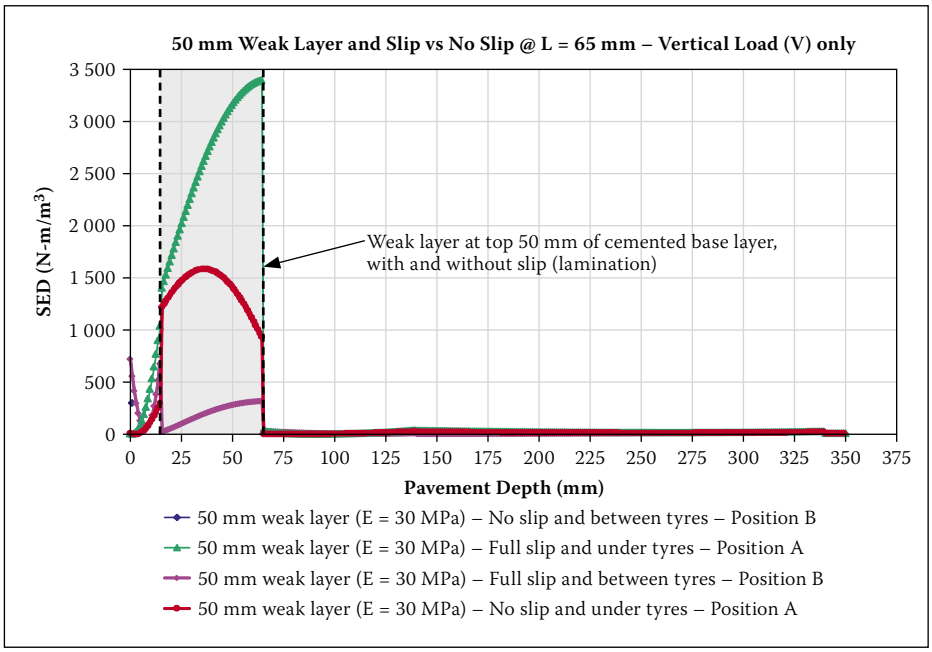

Figure 6 Strain energy of distortion (SED) results of the cemented base pavement for vertical load (V) only. Note the relatively high value of SED at L = 65 mm with full slip (~ single lamination at L = 65 mm) and relatively weak layer (t = 50 mm) on top of the base layer, directly under the tyre

purple curve) was found to be at a position between the dual tyres (Figure 4, Position B), also at the depth of the lamination or weaker interface at L = 65 mm. Most of the other SED values are less than about 25 N-m/m^3. Note that the higher SED values are concentrated in the top 65 mm of the pavement within the base layer, including a "smooth" or full-slip condition at this depth. *This is in sharp contrast to the relatively low SED values (~ 5 N-m/m^3 at 65 mm) found for the ideal case of full friction and no weak interlayer in the base, also indicated in Figure 5 (**blue** and **green** curves). In this case, the maximum SED of approximately 25* N-m/m^3 *is at a depth of 140 mm – at the bottom of the C3 layer (**green** curve).*

It is therefore concluded that the SED of a cemented base layer with "full slip" (lamination or weak interface) peaks directly underneath the tyres (Position A) and is approximately 24 times higher than the case of full-friction (i.e. "no slip" or "rough" or "full bond") condition. This is an analytical demonstration of the potential adverse effect of a lamination or weak interface within the cemented base layer at this depth, as modelled here with SED. This unfavourable condition should be avoided at all times, as it is postulated that it will lead directly to premature *fatigue* failure in the top part of the cemented base pavement. It is probably also associated with the crushing failure of the top ~ 50 mm (discussed above) and hence with potholing in wet conditions. See Photos 3, 5, 6, 9, 11 and 15 in Part 1, and 21, 23, 24 and 25 in this paper (Part 2).

Example 3: Pavement type: cemented base: smooth vs rough single interface within the cemented base, including a relatively weak layer – vertical tyre loading only

In this example, Figure 6 illustrates the SED results of the same cemented base layer pavement discussed above, but including a relatively weak layer of 50 mm thickness (t = 50 mm) in the top part of the base layer. This condition is modelled *with* and *without* a lamination (or weak interface) at the bottom of this weak layer, with depth L = 65 mm. Again, for demonstration purposes only, vertical tyre loading (V) is considered here.

Compared with the results shown in Figure 5, the effect of adding a 50 mm relatively weak layer (modelled here as a layer of relatively low effective elastic modulus of 30 MPa) is quite dramatic. In this case, the maximum SED increased to a value close to 3 500 N-m/m^3, which is approximately 30 times larger (Figure 6) than the case of lamination (full-slip weak interface) only, as shown in Figure 5.

The dramatic 30-fold increase in SED caused by this 50 mm weak layer clearly illustrates the higher potential for distortion (fatigue, rutting or further crushing) that may occur in the top 65 mm of this cemented layer. This, of course, could lead to premature failure, even during the construction period, if such a condition exists. Note also that most of the SED is concentrated in the top part of the cemented base (under the tyres, Position A) where the lamination, weak interface and weak layer are situated. *This is also in sharp contrast to the ideal case of full friction and no weak layer within the base as indicated in Figure 5 (**green** curve), with maximum SED ~ 5 N-m/m^3 at 65 mm.*

Example 4: Effect of horizontal (H) loading – position between the dual tyres (Position B in Figure 4)

To simulate the additional effect of turning/scuffing of tyres around sharp corners or curves, dual tyres with both vertical (V)

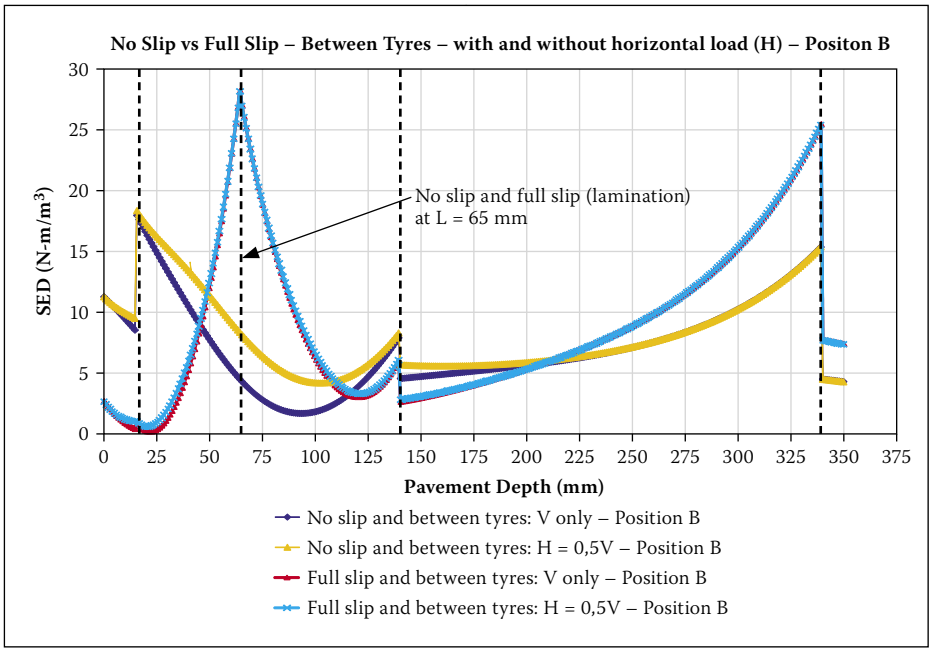

Figure 7 Strain energy of distortion (SED) results of the cemented base pavement midway between the two tyres, with and without horizontal (H) loading. Note the relatively high value of SED at 65 mm with full slip (~ single lamination at L = 65 mm) and the increase in SED on the surface when H-Load is considered under the tyres in addition to vertical (V-Load) only

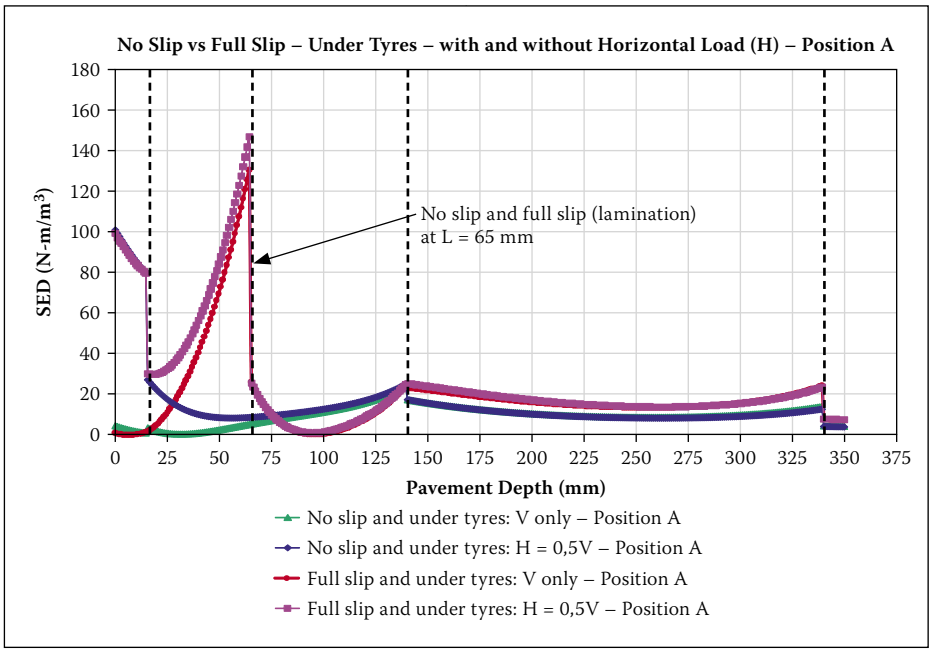

Figure 8 Strain energy of distortion (SED) results of the cemented base pavement under the two tyres, with and without horizontal (H) loading. Note the relatively high value of SED at L = 65 mm with full slip (~ single lamination at L = 65 mm) and the increase in SED on the surface when H-Load is considered under the tyres in addition to vertical (V-Load) only

loading and with and without horizontal (H) loading in the same direction under both tyres, are considered. For demonstration purposes, H was assumed to be about 0,5 of V, i.e. H = 0,5 V (Figure 4). So, with V = 20 kN and H = 10 kN, the pavement was re-analysed in this example. Figure 7 illustrates the effect of SED for the given loading conditions at a position *between* the dual tyres (Figure 4, Position B), and represents a case where no slip ("rough") and full slip (i.e. lamination or weak interface) are considered. Although the SEDs obtained are relatively low for the "no slip" case (**yellow** and dark **blue** curves), the effect of SED can be seen *within* the cemented base layer, peaking at the top and bottom of the layer. Also note the increased SED *within* the cemented base with the horizontal load (compare the **yellow** and dark **blue** curves) between the depths of approximately 15 and 140 mm in Figure 7, suggesting some *additional distortion energies* within the cemented base layer under conditions of horizontal loading between the two tyre loadings. This is a direct result of the horizontal loading under the tyres, which has a potentially adverse effect (increased SED and therefore potentially increased damage) midway between the tyres for the case of no slip (or full friction).

As before, in the case of lamination or a weak interface (full slip) at L = 65 mm, SED peaks at this depth, but with a much-reduced SED of approximately 28 N-m/m^3 (light **blue** and **red** curves), compared with the case under the tyres where the SED was approximately 130 N-m/m^3, shown by the **red** curve in Figure 5. It is interesting to note that at this depth and position midway *between* the tyres (Position B, Figure 4) the additional effect on SED from horizontal loading seems to be relatively small (compare **red** and light **blue** curves in Figure 7).

Example 5: Effect of horizontal (H) loading – position directly under tyres (Position A in Figure 4)

Figure 8 illustrates the SED results *under* one of the dual tyres (Position A). Here the peak SED value is also at the depth of lamination or full slip at L = 65 mm, as before, and is approximately 130 N-m/m^3 for vertical loading only. This value increases to approximately 147 N-m/m^3 if horizontal loading is also included. Note further the increased SED on the *surface* of the pavement, directly under the tyres, from a value of less than 5 N-m/m^3 to approximately 100 N-m/m^3, if horizontal loads are included. This suggests the relatively high potential for *additional* failure potential in the top 65 mm layer under conditions of turning (i.e. "scuffing"), acceleration or deceleration of the tyres on the surface of the pavement. This again shows that a condition of slip in the cemented base layer is to be avoided and, as discussed in Part I, this should be assured through proper inspection during construction and suitable repairs *before* these cemented base layers are sealed.

In Figure 9 the same situation as in Figure 6 (pavement with lamination together with a 50 mm weak layer) is considered, but with the additional horizontal (H) loading included in the analysis. Note the relatively small increase in SEDs compared with those given in Figure 6 for all cases investigated here. Based on the foregoing, it seems that the weak layer in itself overshadows the effect of additional horizontal loading under the tyres in this example. Again, the SED is concentrated in the top part (top 65 mm) of the pavement as modelled here, suggesting shallow failure potential from the top of the layer.

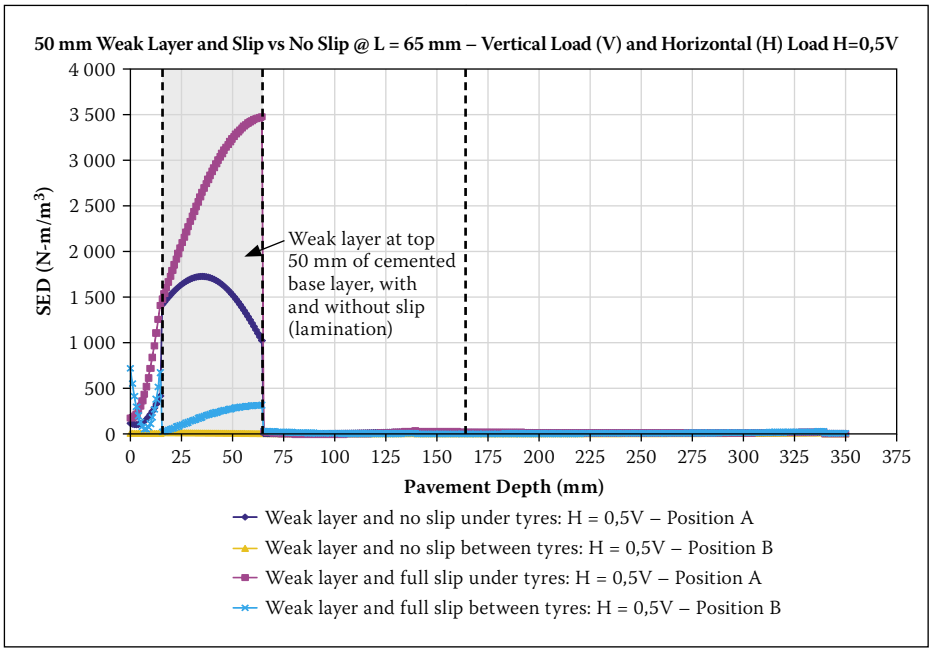

Figure 9 Strain energy of distortion (SED) results of the cemented base pavement for vertical load (V) and horizontal (H) load. Note the relatively high value of SED at L = 65 mm with full slip (~ single lamination at L = 65 mm) and a relatively weak layer (t = 50 mm) on top of the base layer, directly under the tyre (compare with Figure 7 – note the slight increase in SED with H-Load included)

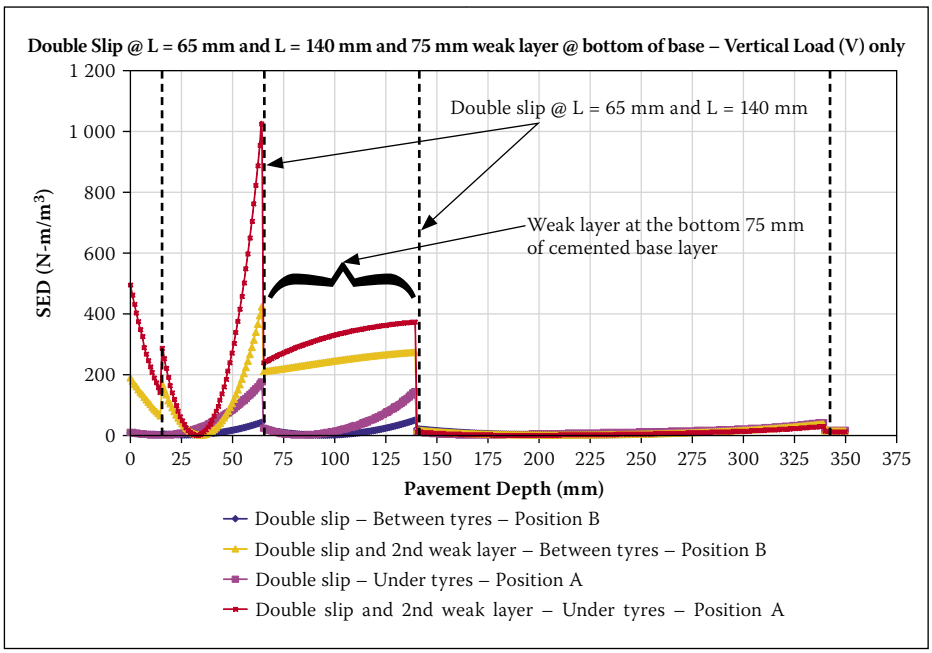

Figure 10 Strain energy of distortion (SED) results of the cemented base pavement. Note the relatively high value of SED at L = 65 mm with full slip (~ double lamination at L = 65 mm and 140 mm) directly under the tyre. Also note the increased effect of SED in the relatively weak layer at the bottom 75 mm of the base

Example 6: Pavement type: cemented base: double slip interfaces – smooth vs rough interfaces within the cemented base, including a relatively weak layer in depth – vertical tyre load only

In this example, the effects of a double slip layer (i.e. two laminations or weak interfaces in the same base layer) at depths L = 65 mm and L = 140 mm, together with a weak layer (due to poor construction, and/or chemical breakdown) between depths of 65 and 140 mm are investigated under vertical tyre loading (V) only. The results are illustrated in Figure 10, which shows the maximum SEDs peaking at the depths of the laminations, i.e. L = 65 mm and L = 140 mm under the tyres (Position A). It is also clear that from a depth of 65 mm, SED increases largely due to the effect of the weak layer, in addition to the two slip layers (compare **red** and **yellow** curves with **purple** and **blue** curves). However, the resulting maximum SEDs under combined conditions of laminations at L = 65 and 140 mm, and the 75 mm thick weak layer at the bottom of the cemented base, appear to be only one third of those obtained for the weak layer only in the top 50 mm and with lamination at L = 65 mm (~ 1 000 N-m/m^3 vs ~ 3 500 N-m/m^3) (Figure 9). Compared to Figure 9, the results in Figure 10 demonstrate the relative importance of a weak layer *directly under the surfacing* seal in the top of the cemented base, accompanied by a slip layer (lamination or weak interface) at its bottom. This finding suggests that the latter case of a shallow weak layer (Figure 9) appears to be *worse* than the case of two laminations and a deeper weak layer towards the bottom of the cemented base (Figure 10).

Example 7: Pavement: granular base on cemented subbases – with and without weak layer and/or slip

In this final example, a relatively strong pavement with a typical high-quality granular (G1 material (COLTO 1996) base layer supported by two lightly cemented layers is investigated. The layout of the pavement and its tyre loading used in the mechanistic analysis are shown in Figure 11. The objective here is to illustrate the effect of a 20 mm relatively weak layer in the top of the upper part of the cemented subbase supporting the G1 base layer by way of analysing the associated SED patterns. First, the pavement was analysed without any weak layer (i.e. solid C3 subbase). The results indicate a peak in SED ~ 100 N-m/m^3 towards the middle of the G1 base layer at a depth of approx. 60 mm (**blue** curve in Figure 12). However, when a 20 mm weak layer is introduced directly underneath the G1 base layer, the SED increases greatly at the bottom of the G1 base layer, as well as within the 20 mm weaker layer (**purple** curve in Figure 12).

From experience, owing to pavement "strength balancing" under the action of tyre loading (or traffic moulding), the G1 granular layer will start to de-densify (or deteriorate) to a relatively lower quality and therefore become a less dense granular layer. This case is modelled here by a reduced effective elastic modulus of 200 MPa (changed from the original 500 MPa (~ G1)), representing a "weakened" G1 granular layer for illustration purposes. The 20 mm weak layer at the top of the upper cemented subbase (C3) is represented here by a weak interlayer (due to poor construction or deleterious chemical breakdown), modelled with an effective elastic modulus of 30 MPa. When the weak layer on top of the subbase, together with this "weakened" G1 base layer, is analysed, the SEDs in the granular

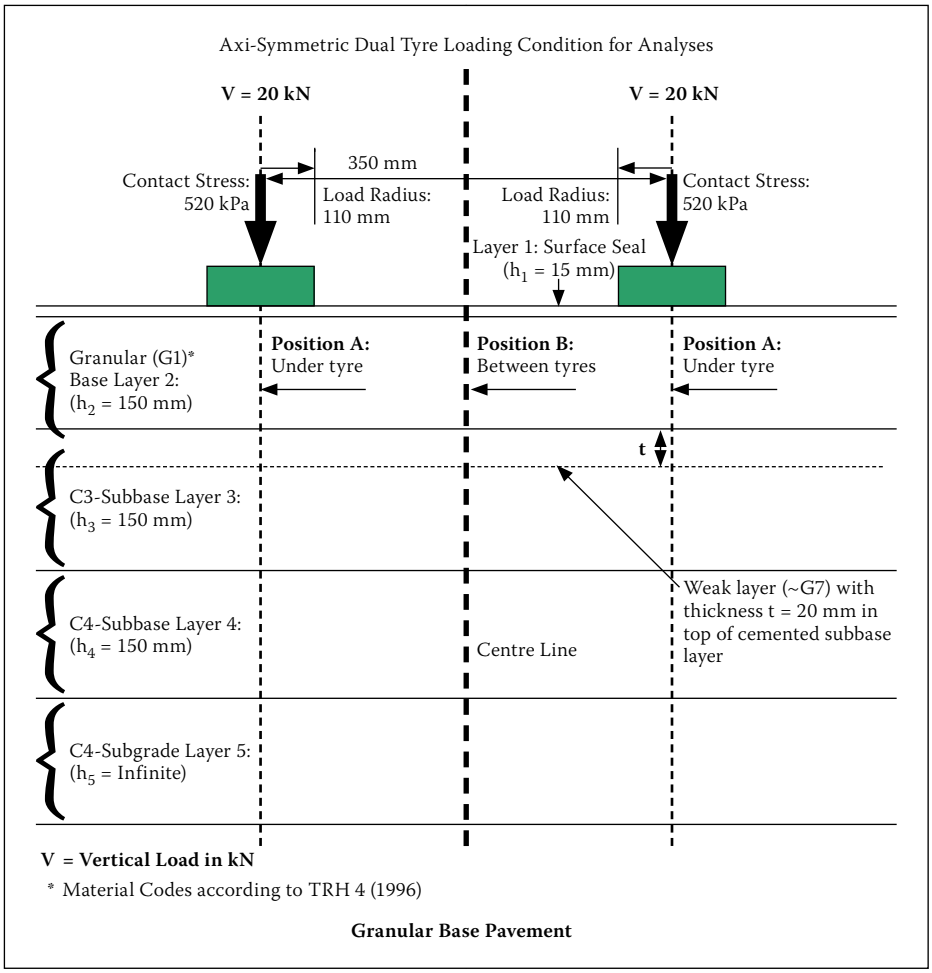

Figure 11 Layout for mechanistic analysis of a high-quality granular (G1-material) base pavement

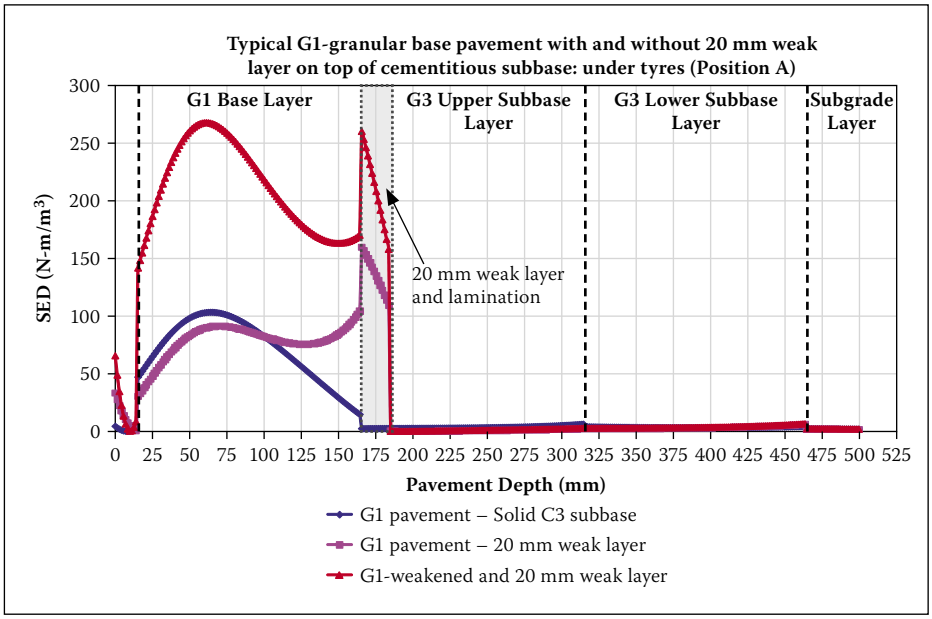

Figure 12 Strain energy of distortion (SED) results of the G1-base (granular) with C3-cemented subbase pavement. Note the relatively high value of SED towards the middle of the granular base layer. Also note the increased SED within and at the bottom of the G1 granular base, as well as within the relatively weak layer at the top 20 mm of the cemented subbase layer at a depth of 165–185 mm. Further note the increased SED within and at the bottom of the (eventually) "weakened" granular layer, and within the 20 mm weak layer

base and the 20 mm weak layer increase to levels almost double those of the case of the 20 mm weak layer only (compare **red** with **purple** curve in Figure 12). Therefore, the adverse effect of a weak layer at the bottom of the G1 layer (or in the top 20 mm of the C3 upper subbase layer) will potentially result in a reduced pavement life, and/or premature failure of the G1 base layer itself. Such a situation could be greatly aggravated when moisture is added to the "weakened" granular base, leading directly to, for example, potholes and base deterioration with further traffic loading. As before, based on the theoretical considerations in this paper, it is therefore concluded that relatively weak layers and interlayers within the supporting structural layers of flexible pavements should be avoided as far as possible in order to ensure quality structural performance of these pavements. It is, however, accepted that further field evaluation and validation are needed to confirm the value of SED as an adequate descriptive mechanistic parameter for the quantification of structural pavement behaviour.

SUMMARY, CONCLUSIONS AND RECOMMENDATIONS

In this paper (Part 2 of the two-part set) it was shown that modelling of flexible and semi-rigid pavements, including weak interlayers, laminations and/or weak interfaces, by way of mechanistic analysis using strain energies of distortion (SED) is quite insightful. In addition, experience and HVS testing have shown that the presence of relatively weak interlayers of any kind (i.e. laminations and/or interlayers of relatively weak quality) is far more deleterious to structural pavement performance than is commonly assumed. Especially the crushing mode of shallow failure and its quantification show good promise for the evaluation and prediction of the structural capacity of pavements incorporating lightly cemented layers under these adverse conditions.

It is concluded that the effects of weak interlayers, laminations and/or weak interfaces can be modelled mechanistically to illustrate and quantify potential failure conditions and their locations. The effect of potential crushing failure of cemented pavement base/subbase layers can also be quantified, albeit empirically. These conditions in the structural pavement layers should (and can) be avoided, especially during construction, in order to ensure quality structural performance of pavements of this nature in the long term.

For the design and modelling of durable flexible and semi-rigid pavements in the context of this paper, the following aspects are recommended:

- In medium to high-risk situations, the mechanistic methodology should include an analysis based on the SED parameter, which may greatly improve engineering understanding of the failure mechanisms, structural behaviour and associated potential for *premature* failure of flexible and semi-rigid pavements. This is

especially important in cases where the upper layers of these pavements may contain weak layers, interlayers, laminations and/or weak interfaces.
- Full-scale pavement studies should be performed and evaluated to calibrate the SED as a potential failure parameter, especially for roads in the conditions described above.
- Emphasis should be placed on ensuring that the construction quality of these pavements is maintained. If a relatively weak layer, interlayer, lamination and/or interface is indeed found in the upper layers of these pavement structures, it should be removed and rectified immediately before any further construction is done, as was discussed in Part 1.
- Pavements incorporating cemented (stabilised) base layers should be evaluated for potential traffic-load-associated crushing failure related to higher tyre contact stresses as proposed in this paper. This is to avoid the shallow crushing failure of these layers when their strength is substandard relative to their strength specifications and the current demand of higher truck tyre contact stresses.

ACKNOWLEDGEMENT

This paper is published with the approval of the Executive Director of the CSIR Built Environment unit.

REFERENCES

Austroads (Association of Australian and New Zealand Road Transport and Traffic Authorities) 1998. Guide to stabilization in roadworks. Austroads Publ. No AP-60/98, Sydney, Australia: Austroads.

COLTO (Committee of Land Transport Officials) 1996. Structural design of flexible pavements for interurban and rural roads. Draft TRH 4: 1996, Pretoria: Department of Transport.

De Beer, M 1985. Behaviour of cementitious subbase layers in bitumen base road structures. MEng dissertation, University of Pretoria, Pretoria.

De Beer, M & Horak, E 1987. The effect of poor drainage on pavement structures studied under accelerated testing. *Proceedings,* Annual Transportation Convention (ATC '87), Pretoria, August, Vol 5B, Paper 5B/1.

De Beer, M 1989a. Compression failure of lightly cementitious materials. Research Report DPVT 36, Pretoria: CSIR Division of Roads and Transport Technology.

De Beer, M 1989b. Dynamic Cone Penetrometer (DCP)-aided evaluation of the behaviour of pavements with lightly cementitious layers. Research Report DPVT 37, Pretoria: CSIR Division of Roads and Transport Technology.

De Beer M & Visser A T 1989. Erodibility of cementitious subbase layers in flexible pavements. *Proceedings,* 5th Conference on Asphalt Pavements for Southern Africa (CAPSA '89), Session VII, Swaziland, 5–9 June, pp VII-1-VII-15.

De Beer, M 1990. Aspects of the design and behaviour of road structures incorporating lightly cementitious layers. PhD thesis, University of Pretoria, Pretoria.

De Beer, M, Fisher, C & Jooste, F J 1997. Determination of pneumatic tyre/pavement interface contact stresses under moving loads and some effects on pavements with thin asphalt surfacing layers. *Proceedings,* 8th International Conference on Asphalt Pavements (8th ICAP '97), Seattle, Washington, US, 10–14 August, Vol 1, pp 179–227.

De Beer, M, Kannemeyer, L & Fisher, C 1999. Towards improved mechanistic design of thin asphalt layer surfacings based on actual tyre/pavement contact stress-in-motion (SIM) data in South Africa. *Proceedings,* 7th Conference on Asphalt Pavements for Southern Africa (CAPSA '99), Victoria Falls, Zimbabwe, 29 August–2 September, Theme 5: Innovation in Asphalt Design.

De Beer, M, Fisher, C & Jooste, F J 2002. Evaluation of non-uniform tyre contact stresses on thin asphalt pavements. *Proceedings,* 9th International Conference on Asphalt Pavements, Copenhagen, Denmark, 17–22 August.

De Beer, M, Fisher, C & Kannemeyer, L 2004. Tyre-pavement interface contact stresses on flexible pavements – quo vadis? *Proceedings,* 8th Conference on Asphalt Pavements for Southern Africa, Roads – The Arteries of Africa, Sun City, South Africa, 12–16 September.

De Beer, M 2006. Reconsideration of tyre-pavement input parameters for the structural design of flexible pavements, *Proceedings,* 10th International Conference on Asphalt Pavements (10th ICAP), Quebec City, Canada, 12–17 August.

De Beer, M 2008. Stress-In-Motion (SIM) – A new tool for road infrastructure protection? *Proceedings,* International Conference on Heavy Vehicles, Paris, France, 19–22 May.

Du Plessis, L, Rust, F C, Horak, E, Nokes, W A & Holland, T J 2008. Cost-benefit analysis of the California HVS Programme. *Proceedings,* 3rd International Conference on Accelerated Pavement Testing (APT '08), Madrid, Spain, 1–3 October.

Freeme, C R 1983. Evaluation of pavement behaviour for major rehabilitation of roads. Research Report RP/19/83, Pretoria: CSIR Division of Roads and Transport Technology.

Freeme, C R & De Beer, M 1983. Companion document to Report RP/19/83 – Evaluation of pavement behaviour for major rehabilitation of roads. Pretoria: CSIR Division of Roads and Transport Technology.

Freeme, C R, De Beer, M & Viljoen, A W 1987. The behaviour and mechanistic design of asphalt pavements. *Proceedings,* 6th International Conference on Structural Design of Asphalt Pavements, Ann Arbor, Michigan, US, 13–17 July, pp 333–343.

Jordaan, G J 1988. Analysis and development of some pavement rehabilitation design methods. PhD thesis, University of Pretoria, Pretoria.

Kleyn, E G, Maree, J H & Terblanche, L J 1985. The impact of Heavy Vehicle Simulator (HVS) testing in the Transvaal. *Proceedings,* Annual Transportation Convention, CSIR, Pretoria.

Lourens, J P 1995. *Towards improved understanding of surfacing, base and tyre interaction for low-cost pavement design.* Research Report RR 93/559, Pretoria: Department of Transport.

Maina, J W, De Beer, M & Matsui, K 2007. Effects of layer interface slip on the response and performance of elastic multi-layered flexible airport pavement systems. *Proceedings,* 5th International Conference on Maintenance and Rehabilitation of Pavements and Technological Control (MAIREPAV5), Park City, Utah, US, 8–10 August.

Maree, J H 1982. Aspekte van die ontwerp en gedrag van padplaveisels met korrelmateriaalkroonlae (Aspects of the design and behaviour of road pavements with granular base layers). PhD thesis, University of Pretoria, Pretoria (in Afrikaans).

Nageim, H Al & Hakim, B Al 1999. Bonding conditions between pavement layers and their influence on pavement layers moduli and remaining life. *Proceedings,* 3rd European Symposium on the Performance and Durability of Bituminous Materials and Hydraulic Stabilised Composites, Leeds, UK, April.

Netterberg, F & De Beer, M 2012. Weak interlayers in flexible and semi-flexible road pavements – Part I. *Journal of the South African Institution of Civil Engineering*, 54(1) (this issue).

Opperman, R A 1984. Die Swaarvoertuignabootsertoetse (SVN toetse) op Pad 30, naby Hornsnek. Technical Research Report RP/3/84, Pretoria: CSIR Division of Roads and Transport Technology (in Afrikaans).

Romanoschi, S A & Metcalf, J B 2001a. Effect of interface condition and horizontal wheel loads on the life of flexible pavement structures. *Transportation Research Record,* 1778: 123–131.

Romanoschi, S A & Metcalf, J B 2001b. Characterization of asphalt concrete layer interfaces. *Transportation Research Record,* 1778: 132–139.

Rust, C R 1987. Load-associated crack movement and aspects of the rehabilitation of reflection cracking in cemented pavements. MEng dissertation, University of Pretoria, Pretoria.

Rust, F C, Kekwick, S V, Kleyn, E G & Sadzik, E S 1997. The impact of the Heavy Vehicle Simulator (HVS) test program on road pavement technology and management. *Proceedings,* 8th International Conference on Asphalt Pavements, Seattle, US, pp 1073–1085.

Steyn, W J vd M 2001. Considerations of vehicle-pavement interaction for pavement design. PhD thesis, University of Pretoria, Pretoria.

Theyse H L, De Beer, M & Rust, F C 1996. Overview of the South African mechanistic pavement design analysis method. *Proceedings,* 75th Annual Transportation Research Board Meeting, Washington, D.C., 7–11 January, Transportation Research Record 1539, pp 6–17.

Timoshenko, S & Goodier, J N 1951. *Theory of Elasticity.* New York: McGraw-Hill.